



## DNPH OF ISOSTEVIOL VIA SIRT 1/ NRF2 SIGNALING PATHWAY ABROGATES NEURONAL SYNAPSE & MEMORY DEFICITS IN AGING MOUSE MODEL

Saif Ullah<sup>1\*</sup>, Muhammad Zahid<sup>2</sup>, Rahmat ali<sup>3</sup>, Muhammad Shimran Khan Afridi<sup>4</sup>,  
Dr. Muhammad Ismail Khan<sup>5</sup>, Shahid Ali Shah<sup>6</sup>, Amir Zeb<sup>7</sup>, Asad Ullah<sup>8</sup>

<sup>1</sup>\*Department of Zoology, Islamia College University, Peshawar, Email: saifk302@gmail.com

<sup>2</sup>Department of Zoology, Islamia College University, Peshawar, Email: drmzahid@icp.edu.pk

<sup>3</sup>Department of Zoology, Islamia College University, Peshawar, Email: Drrahmatali123@gmail.com

<sup>4</sup>Department of Zoology, Islamia College University, Peshawar,  
Email: shimranafridi14@gmail.com

<sup>5</sup>Department of Zoology, Islamia College University, Peshawar, Email: ismail@icp.edu.pk

<sup>6</sup>Department of Biology, Haripur University, Peshawar, Email: shahid.ali@uoh.edu.pk

<sup>7</sup>Department of Natural and Basic Science, University of Turbat, Email: amir.zeb@uot.edu.pk

<sup>8</sup>Department of Chemistry, Islamia College University, Peshawar, Email: asadullah@icp.edu.pk

**\*Corresponding Author:** Saif Ullah

\*Department of Zoology, Islamia College University, Peshawar, Email: saifk302@gmail.com

### ABSTRACT:

Aging is a natural process which can't be stopped and reversed. The physiological changes of aging are inevitable and complex. There are a variety of causatives which speed up this process. The aim of the present study was to find the rational process of aging and to slow down or reverse the molecular intervention in ageing. The current study investigated the neurotherapeutic potential of Dinitrophenyl hydrazine (DNPH) of Isosteviol against D galactose (D-Gal) induced oxidative stress-mediated cognitive deficits in adult albino mice. DNPH of Isosteviol is naturally occurring compound with biological anti-aging properties in adult male albino mice. For a period of eight weeks, intraperitoneal (IP) administration of D-Gal at a dose of 100 mg/kg followed by the administration of DNPH of Isosteviol at a dose of 10 mg/kg on alternating days for the last four weeks. The results have shown that DNPH of Isosteviol significantly restored the cognitive deficits in mice that is assessed with Morris's water maze and Y-maze test. Similarly this DNPH of Isosteviol markedly decreased the oxidative stress induced by D-Gal is determined through various antioxidant assay such as catalase, POD, SOD, glutathione and LPO. Moreover, DNPH of Isosteviol reduced the amyloidogenic pathway of Amyloid beta (A $\beta$ ) to diminish neuroinflammation by decreasing NF-kB and its downstream signaling such as TNF- $\alpha$ . Interestingly, this DNPH of Isosteviol rescued male adult albino mice by stimulating SIRT1 protein to reduce the A $\beta$  production through SIRT1/NRF2/HO-1 signaling pathway.

Taken together, our results suggest that DNPH of Isosteviol is a novel neurotherapeutic agent that can be proved to be a safe, effective in reducing cognitive deficits and other complication associated with aging. A more in detail work is warranted to check the mechanism behind the DNPH of Isosteviol in aging mice.

**Keywords:** DNPH, Isosteviol, SIRT1/NRF2/HO, NFKB, D-Gal.

## INTRODUCTION

The process of aging is multifaceted and results in a progressive deterioration of an organism's physical, mental, and neural capabilities. This decline is caused by alterations in cellular and structural components of the brain, as well as neural processing, cognitive abilities, and behavior. These alterations consist of diminished grey matter, compromised white matter integrity, synaptic dysfunction, and an increased susceptibility to neurodegenerative diseases (Fjell *et al.*, 2014). Annually, a staggering 9.9 million individual's worldwide experience dementia, which serves as a marker of the aging brain (Shwe *et al.*, 2018). Aging is linked to mitochondrial failure, which decreases oxidative phosphorylation and increases free radical and ROS production. (Winklhofer & Haass, 2010). Instead of this, the process of normal aging is linked to a steady and progressive decline in cognitive and physical abilities (Arthur *et al.*, 2009).

However, in neurological illnesses that are influenced by aging, there is a rapid deterioration of cognitive function; leading to significant disturbances in everyday life (Carvalho *et al.*, 2009). Synaptic dysfunction and neuronal loss are two main signs of cognitive decline that comes with getting older. They are caused by changes in how neurons join and change over time (DeKosky & Scheff, 1990). At the end, these problems can make it harder to do daily tasks and make people more likely to get neurodegenerative illnesses like Alzheimer's disease and dementia (Harada *et al.*, 2013).

According to recent studies, continuous D-Gal injection speeds up ageing and affects the cognitive loss that comes with age in mice (Lei *et al.*, 2008). It has been found that mice that received regularly and accurately injected with D-gal for 6-10 week can show signs of natural aging that are used to test anti-aging drugs and study how they work in the body (Zhao *et al.*, 2017). It has been found that the NAD<sup>+</sup>-dependent deacetylases known as Silencing Information Regulator 2 Related Enzyme 1 (SIRT1) is involved in the control of cellular senescence and the advancement of age (Chen *et al.*, 2020). Deacetylation of signal transduction pathway protein substrates regulates gene expression, energy metabolism, cell apoptosis and senescence, inflammation, neuroprotection, the oxidative stress response, and toxicant-induced and SIRT1 activator/inhibitor-antagonized toxic damage (Ren *et al.*, 2019). The SIRT1/NRF2 signaling axis is a crucial regulator of cellular homeostasis and neuroprotection, and it presents potential targets for therapeutic intervention (Zhang *et al.*, 2019; Hwang *et al.*, 2021).

Isosteviol, a naturally occurring chemical extracted from the Stevia plant, has attracted interest due to its potential to protect the nervous system and regulate several cellular pathways associated with ageing and dementia (Chen *et al.*, 2020; Park *et al.*, 2021). Two Isosteviol derivatives, 2,4-dinitro phenyl hydrazine (2,4-DNPH) and 4-nitro phenyl hydrazine (4-NPH), have been made and studied for their good biological activities (Ullah *et al.*, 2019).

This study aims to investigate the neuroprotective properties of DNPH of Isosteviol and its impact on synaptic integrity and memory function in the ageing mice model.

## Material and Methods

This study used adult Albino BAL/B mice were purchased from VRI (Veterinary Research Institute), Peshawar, Pakistan and brought to Neuro Molecular medicines Research Center (NMMRC, Peshawar). The mice were grouped as follows.

1. Normal Mice
2. D-Gal treated (100 mg/Kg) mice
3. D-Gal treated (100 mg/Kg) + DNPH of Isosteviol (10 mg/Kg) treated mice
4. DNPH of Isosteviol treated (10 mg/Kg) mice

All the injections were administered intraperitoneal (i.p.). D-Gal was injected for duration of 8 weeks, while DNPH of Isosteviol was injected during the remaining four weeks. The mice (30–32 g average body weight) were placed in the breeding room with a 12 /12-h light/dark cycle at 25 ± °C

temperature, provided with water and food and libitum. All the work conducted at NMMRC, Peshawar has been authorized by the ethical committee.

### **Behavioral Tests**

Behavioral tests conducted to check the positive effects of DNPH of Isosteviol on D-Gal-induced memory impairment. Adult albino mice were administered D-gal intraperitoneally (i.p.) with or without DNPH of Isosteviol. All mice divided into four groups randomly, and the observer performing the behavioral test was fully unaware of the various mice groups throughout this practice. After the completion of the treatment, the behavioral study of the mice conducted by using the Y-maze test followed by the Morris Water Maze (MWM).

### **Morris Water Maze (MWM) Test**

The MWM test conducted to check the hippocampus-based long-term spatial learning capabilities. The device for MWM testing is described in detail in the recent study (Vorhees *et al.*, 2006). For the first three days, the mice were trained twice daily. The escape latency of the animals to search for the hidden disc observed. If the mice could not locate the platform on their own, they manually guided and made to stay there for 10 seconds. This procedure followed for 5 days; each day, the various experimental groups had a specific set of data (seconds). After receiving two days of rest, the mice subjected to a probe test to search for the hidden disc, and the duration of time they stayed in the target area will be recorded.

### **Y-Maze Test**

This procedure carried out as per the already reported method (Kraeuter *et al.*, 2019). The Y-Maze is a device with three arms that measure 50x10x20cm<sup>3</sup>(LxWxH) and are oriented at 120<sup>0</sup>. Each time, the animals given 10 minutes to acclimatize to their new environment. After that, the animals kept at the center of the maze and given eight minutes to explore the maze. The overall arm entries of the mice and the frequency of the successive triplets monitored using the software. The formula used to calculate the alternations percentage is as follows,

[Spontaneous alternation= Total triplicates/Total arm entries-2] x 100

At the completion of the injections and behavior all the animals were sacrificed and their brain tissue collected carefully. Then these brain tissues were subjected to western blotting and antioxidant enzymes assays techniques.

### **Antioxidant Analysis of Brain Homogenates**

#### **Catalase Assay (CAT)**

For catalase assay, an earlier developed method (Zhang *et al.*, 2017) will be employed with little modifications. The 3 mL reaction mixture comprised 400 μL of 5.9 mM H<sub>2</sub>O<sub>2</sub>, 2500 μL of 50 mM phosphate buffer (at pH 5.0) and 100 μL of brain supernatant. The reaction mixture analyzed for the change in the absorbance at 240 nm at one minute intervals. A 0.01 unit/minute change in absorbance was regarded as one unit of activity.

#### **Reduced Glutathione Assay (GSH)**

The glutathione assay involves the precipitation of proteins contained in 1000 μL of brain homogenate by adding 4% sulfosalicylic acid solution in an equal volume as per previous research (Owen & Butterfield, 2010). After one hour of 4 °C incubation, the reaction mixture was centrifuged for 20 minutes at 1200\*g. The reaction mixture comprised 200 μL of 100 mM DTNB, 100 μL of centrifuged aliquot, and 2700 μL of 0.1 M phosphate buffer at pH 7.4. The change in the absorbance of the reaction mixture immediately measured at 412 nm. Reduced glutathione results expressed as μM/g tissue.

### **Estimation of Lipid Peroxidation (TBARS)**

A previously developed method will be employed (Aguilar & Borges, 2020) with little modification to perform lipid peroxidation assay. This experiment conducted using a 1000  $\mu\text{L}$  of the reaction mixture that contained 20  $\mu\text{L}$  (100 mM) ferric chloride, 200  $\mu\text{L}$  (100 mM) ascorbic acid, 580  $\mu\text{L}$  (0.1 M, pH 7.4) phosphate buffer, and 200  $\mu\text{L}$  brain homogenate supernatant. After 1 hour of incubation at 37 °C, the reaction stopped after adding 1000  $\mu\text{L}$  trichloroacetic acid solution (10%) as a stopping reagent. Then, a 1000  $\mu\text{L}$  thiobarbituric acid solution filled in the tubes, heated to 95°C° for 20 minutes in a hot water bath, and immediately shifted to a crushed ice bath. Subsequent centrifugation for about 10 minutes (at 25\*g) produced lipid peroxidation, calculated from absorbance measured at 535 nm on a spectrophotometer. Results indicated as nM TBARS/min/mg of tissue at a temperature of 37°C (The TBARS molar extinction coefficient is  $1.56 \times 10^5 \text{ M}^{-1} \text{ cm}^{-1}$ ).

### **Peroxidase Assay (POD)**

The POD activity will be measured using the previously described method (de *et al.*, 2021) with little modifications. The mixture used in the current experiment consists of 100  $\mu\text{L}$  of 20 mM guaiacol, 300  $\mu\text{L}$  of 40 mM  $\text{H}_2\text{O}_2$ , 1000  $\mu\text{L}$  brain homogenate supernatant, and 2500  $\mu\text{L}$  of 50 mM phosphate buffer (pH 5.0). The absorbance of the mixture noted at 470 nm at minute intervals. A change of 0.01unit/minute in absorbance taken as one unit of POD activity.

### **Superoxide Dismutase Assay (SOD)**

An earlier developed method will be employed (McCord *et al.*, 1969) with slight modification to perform a superoxide dismutase assay. For this purpose, the reaction mixture comprised 300  $\mu\text{L}$  brain homogenate supernatant, 1200  $\mu\text{L}$  of 0.052 mM sodium pyrophosphate buffer (pH 7.0), and 100  $\mu\text{L}$  (186 M) phenazine methosulphate. The enzymatic process will be initiated after adding 200  $\mu\text{L}$  of 780 mM NADH to the reacting mixture. The reaction stopped after adding 1000  $\mu\text{L}$  of glacial acetic acid at an interval of 1 minute. The absorbance of the mixture noted at 560 nm, and the amount of chromogen produced were quantified in units per mg of protein.

### **Western Blotting Analysis**

Following the duration of treatment, the animals were sacrificed to conduct the western blot analysis, as previously reported (Fido *et al.*, 1995). The mice brains were immediately recovered and carefully separated, immersed in a 1:1 RNA-to-PBS solution on ice. Afterward, the brain component blended with a T-PER (Thermo Scientific) reagent to extract the protein from the tissue. To determine the protein concentration, Bio-Rad protein assay tests performed to measure absorbance at 595 nm. The protein of each sample standardized to 30 $\mu\text{g}$ /group, and an electrophoresis gel of 12 to 15% SDS PAGE was used. It was then followed by transferring protein samples onto the PVDF membrane (Santa Cruz Biotechnology, Santa Cruz, CA, USA) using a semi-dry transblot (Bio-Rad). Various primary antibodies i.e., mouse-derived (anti-actin, anti-SYP, anti-SIRT1, anti-NRF-2, anti-HO-1, anti-A $\beta$ , anti-BACE1, anti-TNF- $\alpha$  and anti-PSDF95) monoclonal antibodies (Santa Cruz, CA, USA) were used. Finally, HRP conjugated anti-mouse secondary antibody (Santa Cruz, CA, USA) used, and the X-ray based results developed carefully.

### **Molecular Docking**

The binding affinity of Sirtuin 1 (SIRT1) in complex with 2,4-Dinitrophenylhydrazine (DNPH) was predicted by molecular docking simulation. Schrodinger Maestro has an inbuilt module “Glide”, which is reliably uses for molecular docking of protein-ligand complex (Rana *et al.*, 2020; Irfanullah *et al.*, 2018). Herein, the experimentally determined structure of SIRT1 in complex with Sirtuin activating compound (STAC) was obtained from protein data bank (PDB ID: 4ZZJ) (<https://www.rcsb.org/structure/4ZZJ>).

Before conducting docking simulation, the structure of SIRT1 in complex with inbound substrate peptide,  $\text{NAD}^+$  and STAC was pre-processed by removing all the solvent and other co-crystallized

unwanted moieties. The cleaned structure of SIRT1 was energy minimized to the local minima by *protein preparation wizard* module implanted in Schrodinger Maestro. Herein, the energy minimization was performed by using the OPLS4 forcefield and conjugate gradient and steepest descent algorithms. Subsequently, the target ligand “2,4-Dinitrophenylhydrazine” (hereafter DNPH) was created and optimized for docking by employing the *LigPrep* module implanted in Schrodinger Maestro.

Thenceforth, the docking grid was generated by selecting the inbound STAC in the N-terminal domain (NTD) of SIRT1, which is occupied the allosteric activation site of SIRT1. The docking grid was generated by using the *Receptor Grid Generation* protocol. Further, the previously prepared SIRT1 structure and DNPH were employed as receptor and ligand input files for docking simulation by the *Glide Docking* module. In brief, the docking protocol was designed as the total numbers of conformers were set to 50, while the total number of poses for output file was set to 40. The docking algorithm was set to standard precision (SP) docking scoring function to ensure the high level of accuracy. The rest of docking parameters were executed as default values.

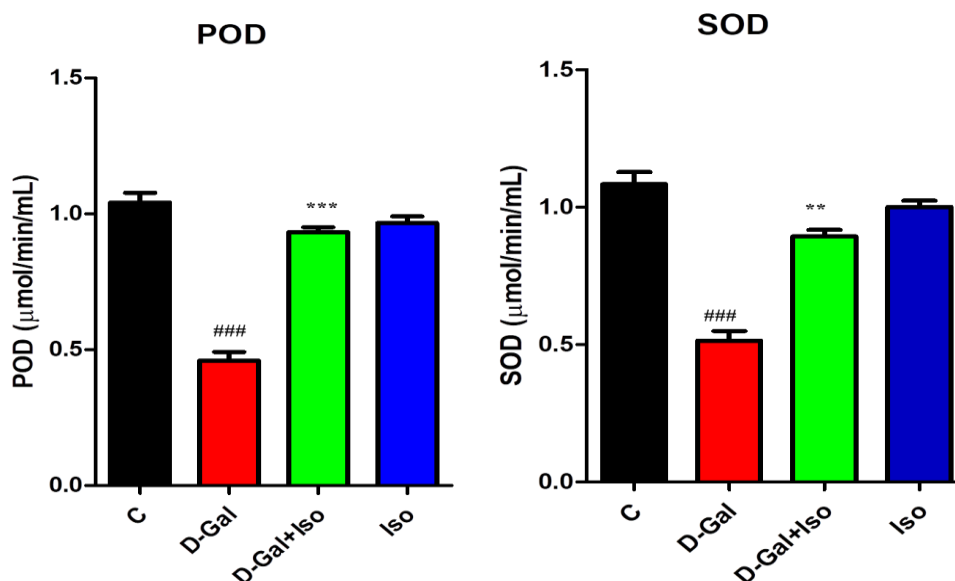
### Statistical Analysis

Every X-ray of the results was scanned, gathered, and statistically analyzed using designated computer-based programmes. Among them are Adobe Photoshop, Prism 5 graph pad, and picture J. Protein density is given in arbitrary units (A.U.s.) as the mean  $\pm$  S.E.M. # substantially different from normal saline treated mice and \* significantly different from D-Gal-treated mice respectively; \*\*### P < 0.01.

## RESULTS

### DNPH of Isosteviol Reduced D-Gal-Induced Oxidative Stress in Mice Brain.

D-Gal induces excessive accumulation of ROS (reactive oxygen species) that leads to oxidative stress (Kumar *et al.*, 2022). Thus, our findings have evaluated the ant oxidative stress capability of DNPH of Isosteviol against D-Gal-Induced oxidative stress in the mice brain. After treatment with DNPH of Isosteviol all the brain homogenates were subjected to the antioxidant assay like POD, SOD, catalase (CAT), glutathione (GSH) and LPO (lipid peroxidation). The results showed that D-Gal inhibited the activities of antioxidant enzymes such as POD, SOD, CAT, GSH and increased LPO activities. On the other hand the administration of DNPH of Isosteviol significantly restored the antioxidant activities of enzymes and also decreased oxidative stress, suggesting an enhanced antioxidant capacity of DNPH of Isosteviol to protect the brain against D-Gal-Induced oxidative damage. The POD, SOD, CAT, LPO, and GSH activities are shown in **Fig.1 (A-E)** respectively.



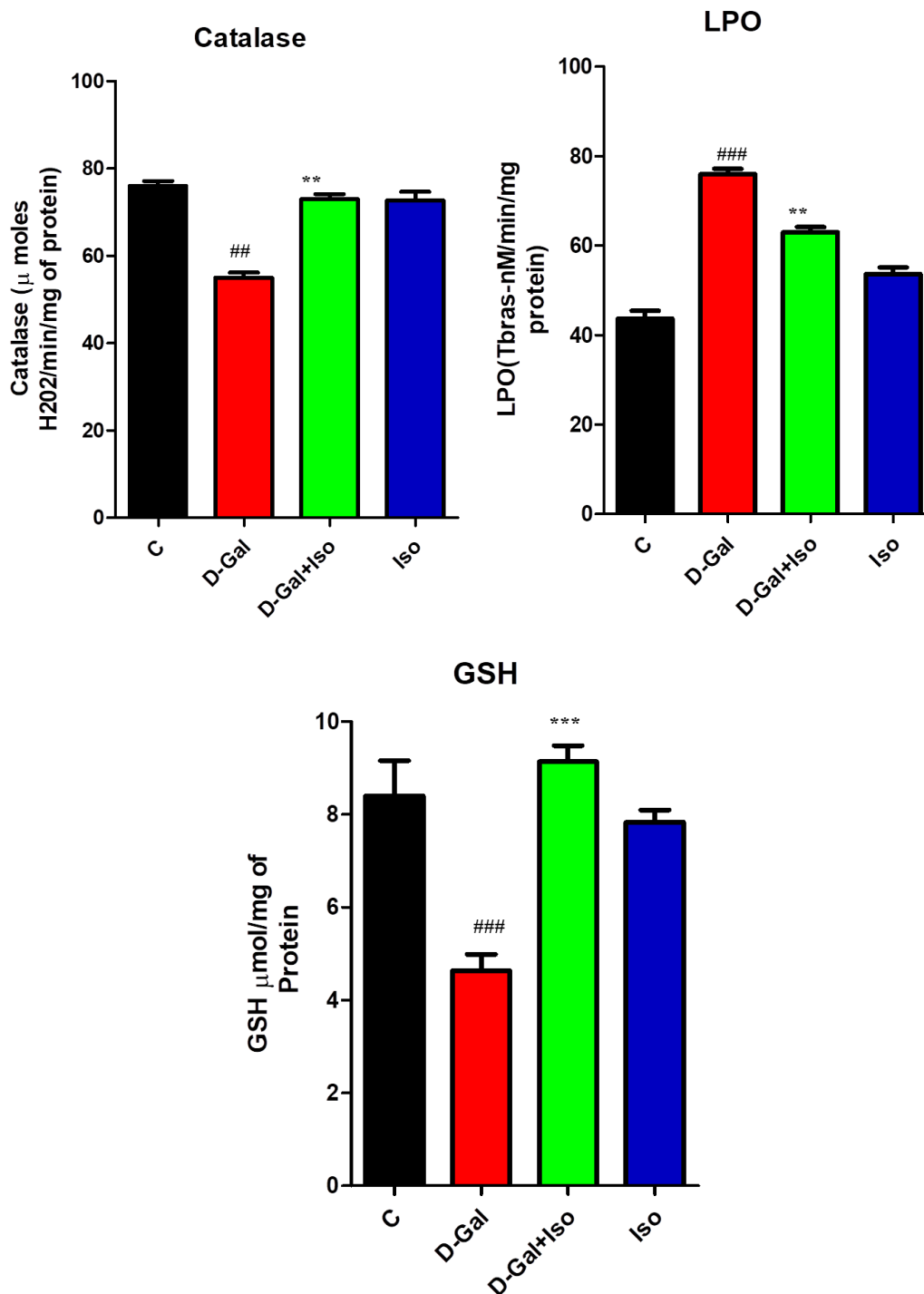


**Figure 1: DNPH of Isosteviol reduced D-Gal-induced oxidative stress in adult mice brain.** Here are the graphs displaying the results of antioxidant enzyme assays. The assays were performed with brain homogenates from four groups of mice: control, D-Gal treated, D-Gal plus DNPH of Isosteviol treated, and DNPH of Isosteviol alone treated. The enzymes catalase, lipid peroxidase (TBARS), glutathione (GSH), and superoxide dismutase (SOD) were added. All of these tests were run three times, and the specifics of the treatments used are detailed in the "materials and methods" section. Mean  $\pm$  SEM of five mice per group is how the results are presented. \*Denotes the comparison of D-Gal with D-Gal + DNPH of Isosteviol, while # indicates the significance of control compared to D-Gal. Determination of significance: ##, \*\*  $p \leq 0.01$  and ###, \*\*\*  $p \leq 0.001$ .

**DNPH of Isosteviol Abrogate D-Gal-induced A $\beta$  Production in Mice Brain.**

D Gal is known for inducing A $\beta$  production in the brain of mice (Shwe *et al.*, 2018). For this reason, we also investigated the amyloid beta production pathway in D galactose induced aging mice model. Our result reveals that D-Gal caused a significant increase in the expression of BACE1 (Beta amyloid cleaving enzyme1) which acts on amyloid precursor protein (APP) to cleave it in three positions i.e., to produce toxic amyloid beta fragments thus increase the maximum production of A $\beta$  and hence increase its deposition. As shown in **figure 2(A-C)**. On the other hand, the administration of DNPH of Isosteviol significantly inhibited BACE1 accompanied by less production of A $\beta$ . This has been depicted in **fig.2 (A-C)**

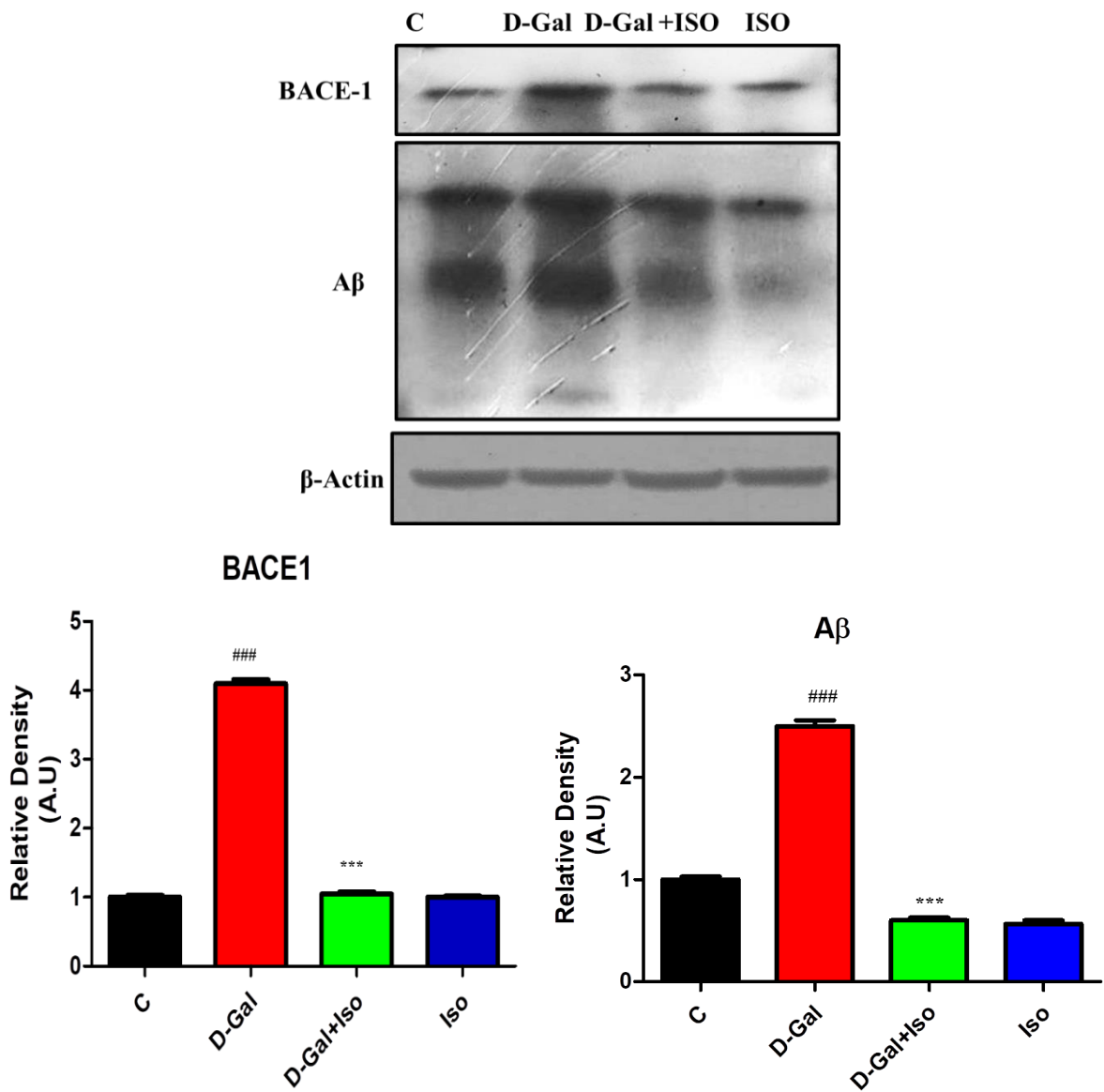


**Figure 2: DNPH of Isosteviol inhibited BACE1 proteins to reduce A $\beta$  expression against D-Gal in mice.** (A) This is an illustration of the western blot results showing the expression of the BACE1 and A $\beta$  proteins in the brain supernatant of mice that were either treated with D-Gal alone or with DNPH of Isosteviol together. (B, C) Here we can see the histograms of the two relative density distributions. In order to determine densities and create graphs, the Image J program was utilized. The data were presented in arbitrary units (A.U.) and calculated using a histogram that shows the mean in A.U  $\pm$  SEM. Both  $p \leq 0.01$  and  $p \leq 0.001$  are noteworthy.

### DNPH of Isosteviol attenuated D-Gal induced Neuroinflammation.

D-Gal is known for inducing neuroinflammation in the brain of mice (Ahmad *et al.*, 2021). To investigate this matter, we observed that the D-Gal caused the induction of TNF alpha as a neuroinflammatory protein marker as shown in the figure 3. In contrast to this the DNPH of Isosteviol significantly reduced the TNF alpha as a neuroinflammatory protein marker as shown in the figure 3(A,B)

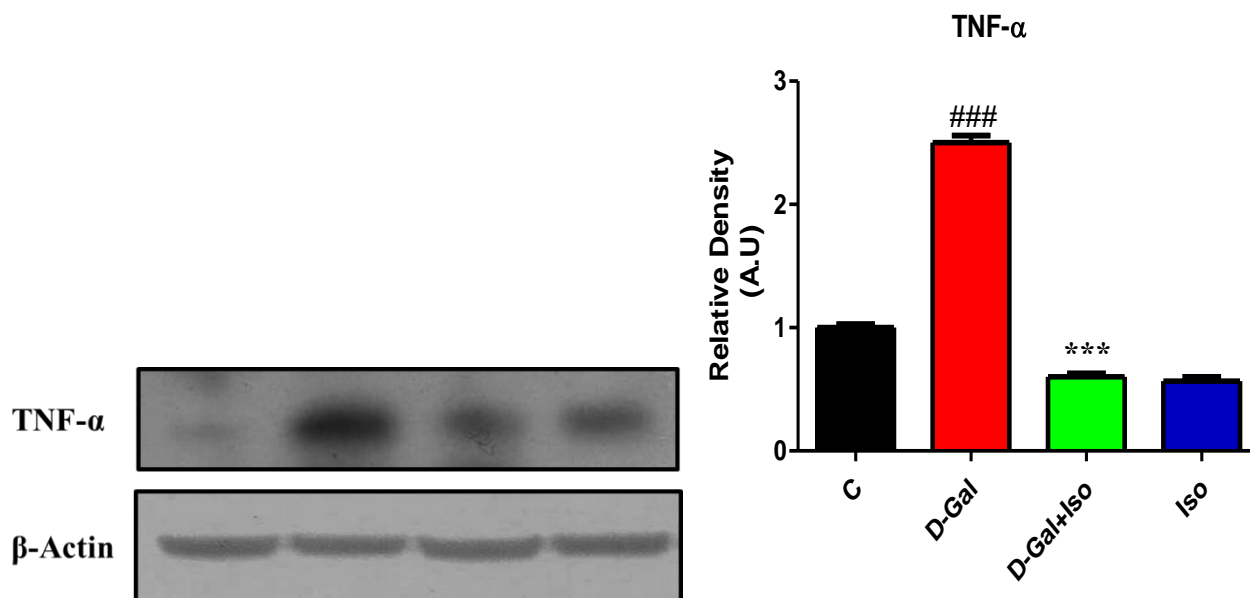


Figure 3: DNPH of Isosteviol attenuated Neuroinflammation against D-Gal in mice.

The western blot result of the TNF- $\alpha$  protein expression in the brain supernatant of mice homogenates treated with D-Gal alone or in combination with DNPH and Isosteviol is displayed in (A). In figure B, Here we can see the histogram of the relative densities. In order to determine densities and create graphs, the Image J program was utilized. The data were presented in arbitrary units (A.U.) and calculated using a histogram that shows the mean in A.U  $\pm$  SEM. Significance:  $p \leq 0.01$  and  $p \leq 0.001$ .

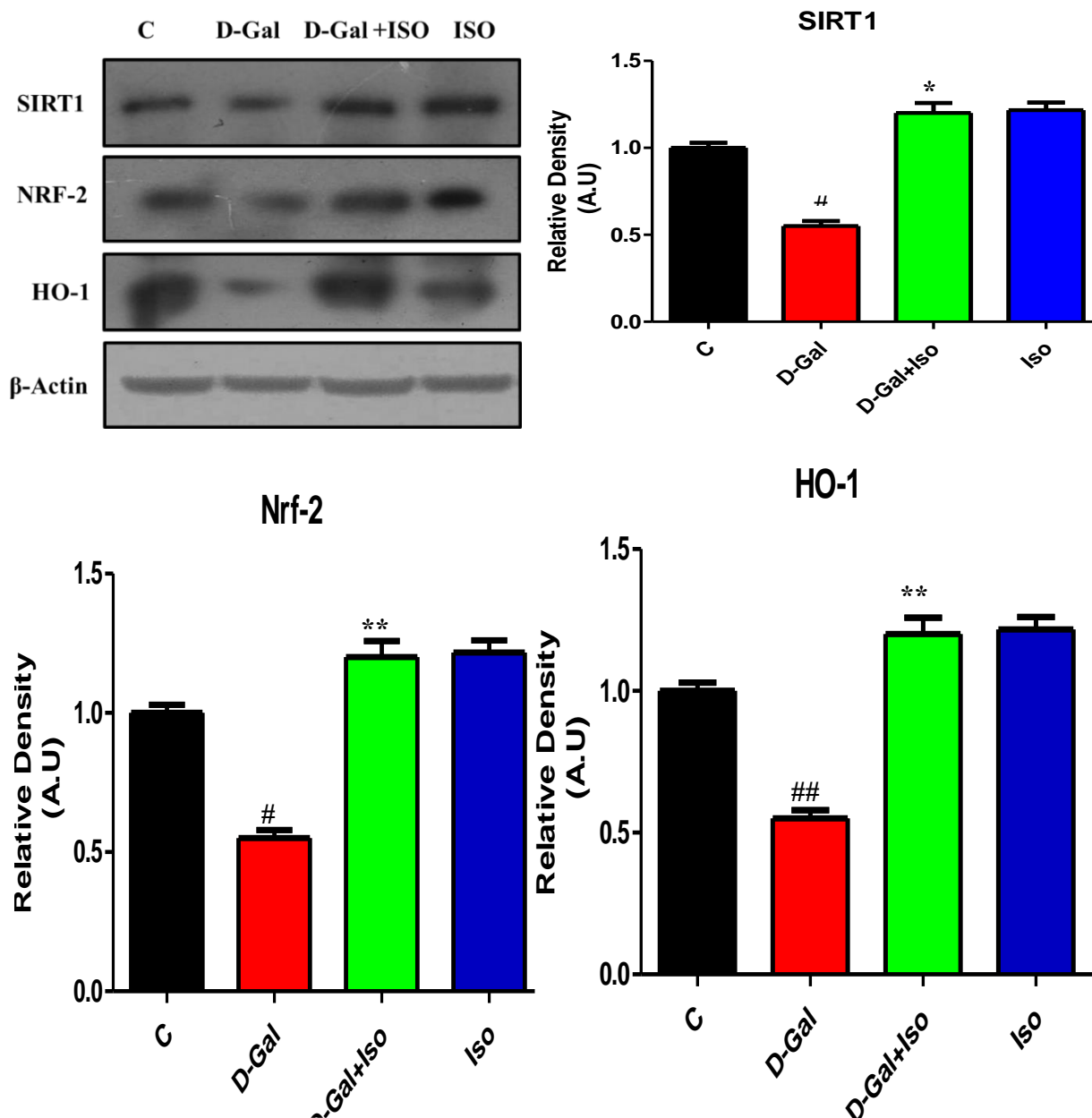
### DNPH of Isosteviol stimulated SIRT1/Nrf-2/HO-1 signaling pathway in Mice.

It has been now well documented that D-gal is causing oxidative stress when chronically injected to mice or rats (Parameshwaran *et al.*, 2010). Due to oxidative stress burden the antioxidant defense molecules of the body such as SIRT1 and NRF-2/HO-1 are suppressed and cannot perform their normal functioning (Hammad *et al.*, 2023). For this reason we have evaluated the expression levels of SIRT1 and NRF-2/HO-1 through western blotting. The western blot results indicate that chronic administration of D- D-Gal to mice significantly inhibited SIRT1, NRF-2 and HO-1 proteins in the brain homogenates of the experimental animals. Interestingly, DNPH of Isosteviol supplementation to the mice in combination with D-Gal enhanced and activated the anti-oxidant proteins such as SIRT1, NRF-2 and HO-1 against D-Gal induced oxidative stress as given in the figure 4(A-D).

The docking of DNPH in the allosteric binding site of SIRT1 suggested that DNPH occupied the allosteric binding site in the N-terminal domain (NTD) of SIRT1 and oriented the same conformation which was reported for the previously identified Sirtuin1 activating compounds (STACs) (Fig. 1A, B) (Dai *et al.*, 2015, Cao *et al.*, 2015, Azminah *et al.*, 2019). Our docking results also suggested that the dinitro moiety of the DNPH is pointed to the shallow regions formed by the major groove of NTD in SIRT1 (Fig. 1B). Further, a nitro (NO<sub>2</sub>) group at position 2 of phenyl ring has established two hydrogen bonds with threonine 219 (T219) and glutamine 222 (Q222) residues of SIRT1 as shown in figure 1C and D. In parallel, the other nitro at position 4 of phenyl ring has formed a single hydrogen bond with the asparagine 226 (N226) residue of SIRT1 (Fig. 1C, D). Our



docking results observed that the orientation of DNPH is nearly similar to other SIRT1 activators by facing the substrate binding site of SIRT1 (Dai *et al.*,2015, Azminah *et al.*, 2019). Therefore, we argue that DNPH may follow the same mechanism of activation of SIRT1 like other STACs. Following the binding stability of DNPH and SIRT1, the 2D interaction pattern of DNPH displayed several hydrophobic interactions with the residues forming the allosteric binding site of SIRT1, leveraging strong binding affinity of SIRT1 and DNPH (Fig. 4E).



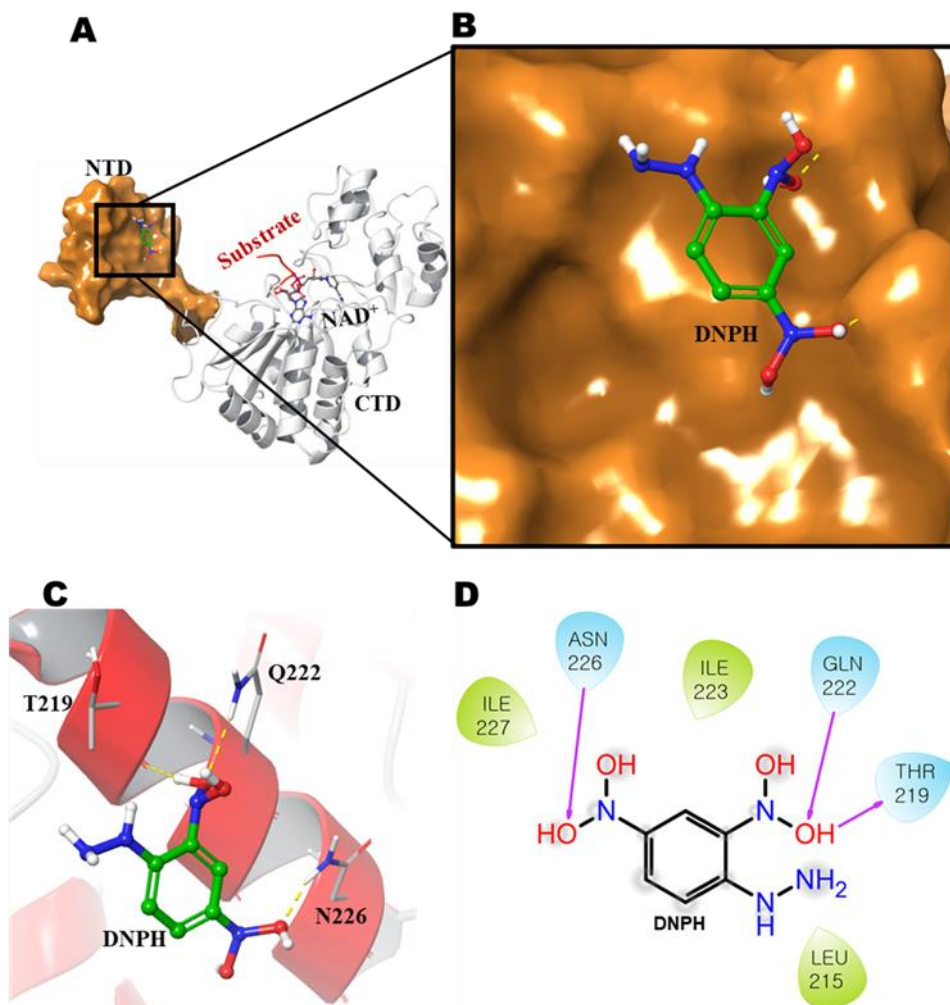


**Fig. 4. DNPH of Isosteviol attenuated D-Gal induced oxidative stress via SIRT1/NRF-2/HO-1 signaling pathway in mice brain.** (A)The western blot analysis of post-treatment brain homogenates of mice was used to examine the protein expression of SIRT1, NRF-2, and HO-1. The  $\beta$ -actin serves as a reference control in all proteins. (B-D) Protein bands were

quantified using Image J software. We used one-way ANOVA and the student's t test for all of our statistical analyses. **Figure 1: Docking of SIRT1 with DNPH.** A) Shows the SIRT1 in complex with DNPH, inbound substrate peptide, and nicotinamide adenine dinucleotide ( $\text{NAD}^+$ ). NTD and CTD stands for N-terminal and C-terminal domains, respectively. DNPH accommodated the allosteric binding site of SIRT1. B) Zoom in view of DNPH orientation in the allosteric binding site of SIRT1. C) Shows the 3D interaction pattern of DNPH in the allosteric binding site of SIRT1. The DNPH is displayed as stick representation with carbon atoms as green colored. The interacting residues of SIRT1 are depicted as thin stick representation with carbon atoms as light gray colored and labelled. The hydrogen bonds are represented as yellow dashed-lines. D) The 2D interaction pattern of DNPH and SIRT1, the hydrogen bonds, and other hydrophobic interacting residues are displayed. The hydrogen bonds are portrayed as magenta colored arrow lines. The densities of the bands are given in arbitrary units (AUs) as the mean  $\pm$  S.E.M. #significantly different from normal saline treated and \*significantly different from D-gal-treated rats respectively; \*#  $P < 0.01$ .

quantified using Image J software. We used one-way ANOVA and the student's t test for all of our statistical analyses. **Figure 1: Docking of SIRT1 with DNPH.** A) Shows the SIRT1 in complex with DNPH, inbound substrate peptide, and nicotinamide adenine dinucleotide ( $\text{NAD}^+$ ). NTD and CTD stands for N-terminal and C-terminal domains, respectively. DNPH accommodated the allosteric binding site of SIRT1. B) Zoom in view of DNPH orientation in the allosteric binding site of SIRT1. C) Shows the 3D interaction pattern of DNPH in the allosteric binding site of SIRT1. The DNPH is displayed as stick representation with carbon atoms as green colored. The interacting residues of SIRT1 are depicted as thin stick representation with carbon atoms as light gray colored and labelled. The hydrogen bonds are represented as yellow dashed-lines. D) The 2D interaction pattern of DNPH and SIRT1, the hydrogen bonds, and other hydrophobic interacting residues are displayed. The hydrogen bonds are portrayed as magenta colored arrow lines. The densities of the bands are given in arbitrary units (AUs) as the mean  $\pm$  S.E.M. #significantly different from normal saline treated and \*significantly different from D-gal-treated rats respectively; \*#  $P < 0.01$ .

quantified using Image J software. We used one-way ANOVA and the student's t test for all of our statistical analyses. **Figure 1: Docking of SIRT1 with DNPH.** A) Shows the SIRT1 in complex with DNPH, inbound substrate peptide, and nicotinamide adenine dinucleotide ( $\text{NAD}^+$ ). NTD and CTD stands for N-terminal and C-terminal domains, respectively. DNPH accommodated the allosteric binding site of SIRT1. B) Zoom in view of DNPH orientation in the allosteric binding site of SIRT1. C) Shows the 3D interaction pattern of DNPH in the allosteric binding site of SIRT1. The DNPH is displayed as stick representation with carbon atoms as green colored. The interacting residues of SIRT1 are depicted as thin stick representation with carbon atoms as light gray colored and labelled. The hydrogen bonds are represented as yellow dashed-lines. D) The 2D interaction pattern of DNPH and SIRT1, the hydrogen bonds, and other hydrophobic interacting residues are displayed. The hydrogen bonds are portrayed as magenta colored arrow lines. The densities of the bands are given in arbitrary units (AUs) as the mean  $\pm$  S.E.M. #significantly different from normal saline treated and \*significantly different from D-gal-treated rats respectively; \*#  $P < 0.01$ .

quantified using Image J software. We used one-way ANOVA and the student's t test for all of our statistical analyses. **Figure 1: Docking of SIRT1 with DNPH.** A) Shows the SIRT1 in complex with DNPH, inbound substrate peptide, and nicotinamide adenine dinucleotide ( $\text{NAD}^+$ ). NTD and CTD stands for N-terminal and C-terminal domains, respectively. DNPH accommodated the allosteric binding site of SIRT1. B) Zoom in view of DNPH orientation in the allosteric binding site of SIRT1. C) Shows the 3D interaction pattern of DNPH in the allosteric binding site of SIRT1. The DNPH is displayed as stick representation with carbon atoms as green colored. The interacting residues of SIRT1 are depicted as thin stick representation with carbon atoms as light gray colored and labelled. The hydrogen bonds are represented as yellow dashed-lines. D) The 2D interaction pattern of DNPH and SIRT1, the hydrogen bonds, and other hydrophobic interacting residues are displayed. The hydrogen bonds are portrayed as magenta colored arrow lines. The densities of the bands are given in arbitrary units (AUs) as the mean  $\pm$  S.E.M. #significantly different from normal saline treated and \*significantly different from D-gal-treated rats respectively; \*#  $P < 0.01$ .

quantified using Image J software. We used one-way ANOVA and the student's t test for all of our statistical analyses. **Figure 1: Docking of SIRT1 with DNPH.** A) Shows the SIRT1 in complex with DNPH, inbound substrate peptide, and nicotinamide adenine dinucleotide ( $\text{NAD}^+$ ). NTD and CTD stands for N-terminal and C-terminal domains, respectively. DNPH accommodated the allosteric binding site of SIRT1. B) Zoom in view of DNPH orientation in the allosteric binding site of SIRT1. C) Shows the 3D interaction pattern of DNPH in the allosteric binding site of SIRT1. The DNPH is displayed as stick representation with carbon atoms as green colored. The interacting residues of SIRT1 are depicted as thin stick representation with carbon atoms as light gray colored and labelled. The hydrogen bonds are represented as yellow dashed-lines. D) The 2D interaction pattern of DNPH and SIRT1, the hydrogen bonds, and other hydrophobic interacting residues are displayed. The hydrogen bonds are portrayed as magenta colored arrow lines. The densities of the bands are given in arbitrary units (AUs) as the mean  $\pm$  S.E.M. #significantly different from normal saline treated and \*significantly different from D-gal-treated rats respectively; \*#  $P < 0.01$ .

#### DNPH of Isosteviol restored neuronal synapse deficits in adult Mice.

D-Gal is known to induce synaptic as well as memory dysfunction in animal model of mice or rat (Samad *et al.*, 2022). Similarly in the current study we also observed that this D Galactose caused synaptic deficits both (pre- and post-) synapse of mice brain homogenate is assessed by western blot analysis as shown in figure. On the other side while animals received DNPH of Isosteviol in

combination with D-Galactose have shown improved DNPH of Isosteviol restored neuronal synapse in Mice. Neuronal synapse as depicted in western blot in **fig.5(A-C)**

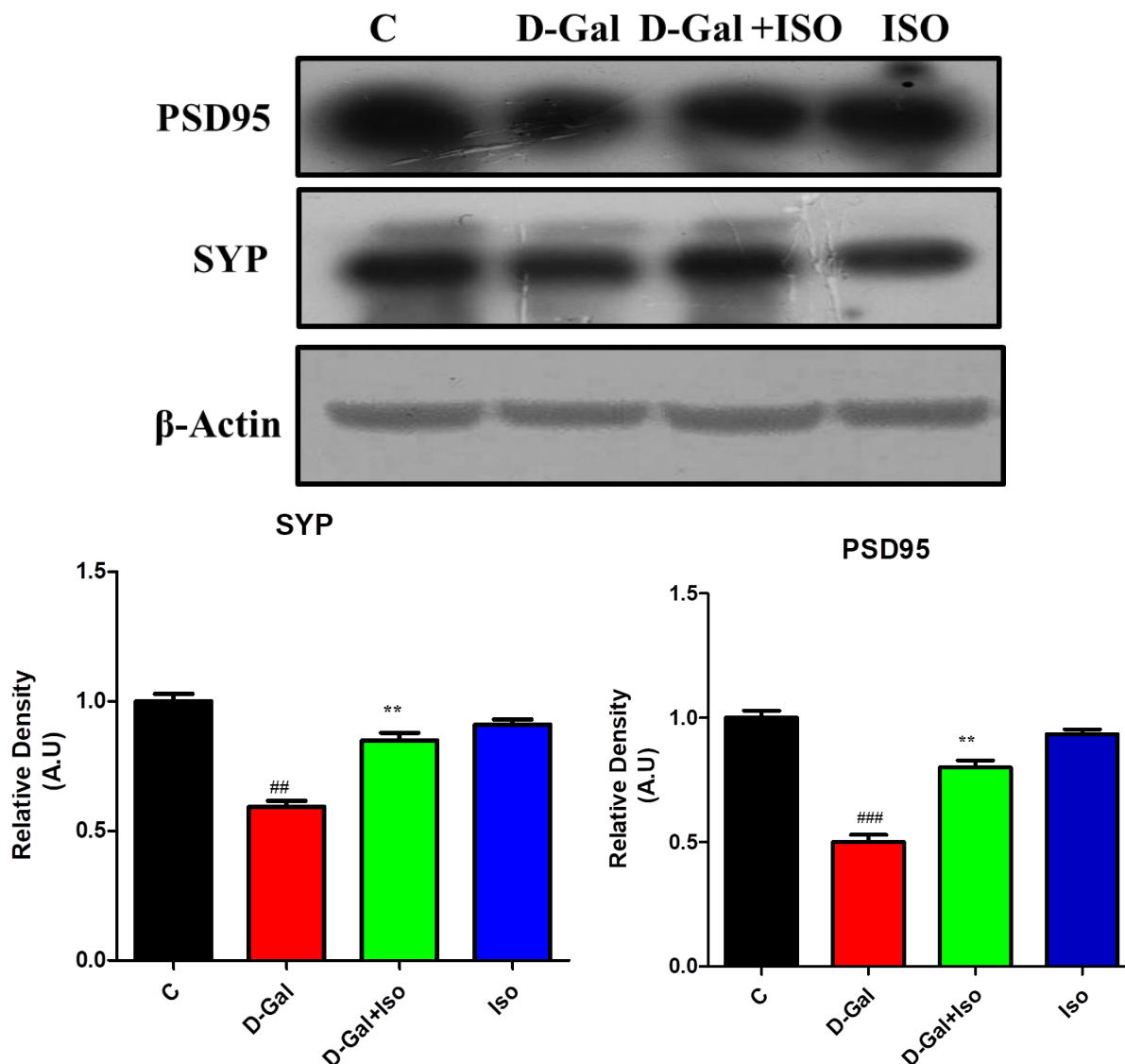


**Figure 5. DNPH of Isosteviol enhanced synaptic decline against long time administration of D-gal in mice brain.** (A) Shown are the Western blot results of both pre- and post-synapse proteins (SYP and PSD95) along with their respective histograms (B,C) of all the three experimental groups (n=5/group). Image J a computer based software was used for the quantification of the protein bands.  $\beta$ -actin was used as a house keeping gene. Graph pad Prism 5 was used to make the histograms and for all the statistical analysis through one way ANOVA followed by student's t test. The density of proteins is expressed in arbitrary units (A.U.s) as the mean  $\pm$  S.E.M. #significantly different from normal saline treated and \*significantly different from D-gal-treated mice, respectively; ### P < 0.01.

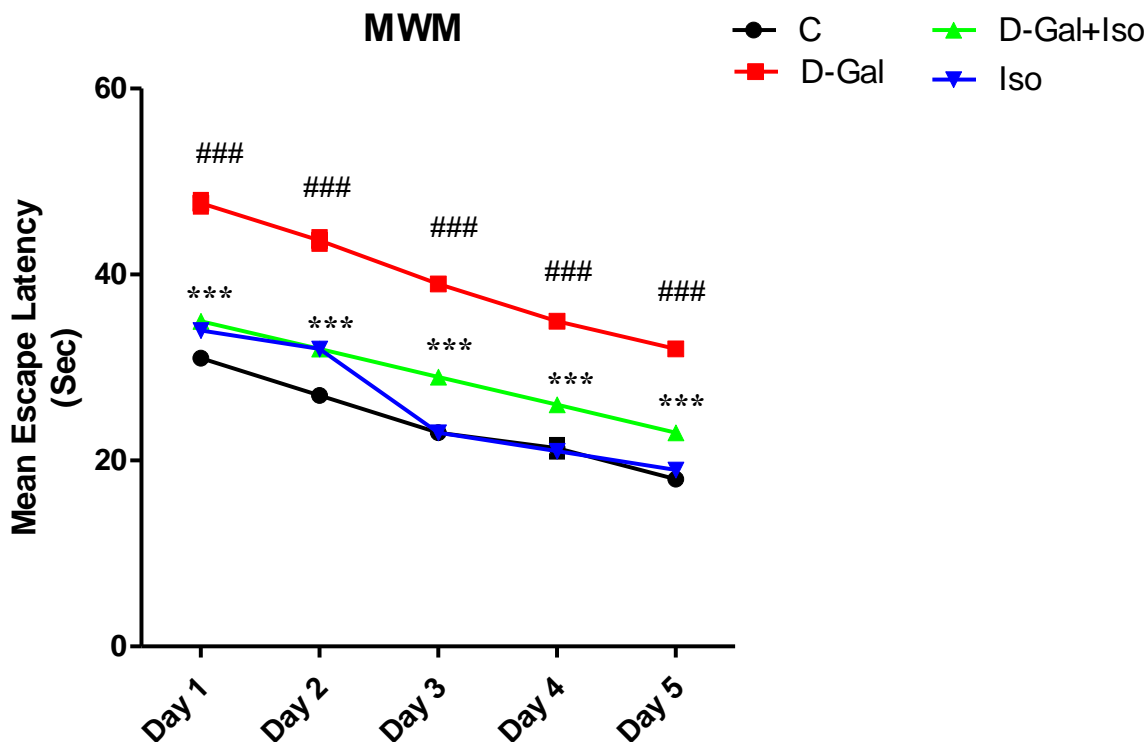
### DNPH of Isosteviol improved Memory and Behavior in D-gal treated Mice

The effect of DNPH of Isosteviol on spatial learning and memory was analyzed through Morris water maze and Y-maze in D-gal administered ageing model. These mice were first trained, rested and then their data was collected on day 1 until to 5th day. As per our results which indicate that the mean latency to locate the submerged platform in all the experimental groups decreased slowly during the training days. On day 1 the D-gal treated mice did not find the submerged platform, while the DNPH of Isosteviol treated mice find it and escaped. Similarly, on day 2 and following days the

D-gal treated mice succeeded in finding the submerged platform but their escape latency (seconds) was very high. Interestingly, DNPH of Isosteviol treated mice showed good learning abilities and their escape latencies were significantly ( $P < 0.01$ ) decreased in finding the submerged platform from day 2 to day 5 and almost equals to the normal mice. The normal mice were observed to have very low escape latency and there escape latency was reduced from day 1 to 5th day as given in the figure A. As shown in the figure 2A that, only D-gal-treated mice exhibited longer latencies to the submerged platform in comparison to the normal mice. These findings indicate that the spatial learning impairment and memory dysfunction in D-gal-administered mice. In contrast to that the mice received DNPH of Isosteviol (10 mg/kg) injections along with D-gal significantly ( $P < 0.01$ ) reduced the increased latencies to the platform in treated mice Fig. 6(A-C).

On day 6 when the submerged platform was removed and the respective time spent in the target quadrant was observed of all the three groups. The mice were then allowed to find the hidden submerged platform. The data taken indicate that control animals spent more time in the target quadrant while D-gal treated mice spent less time in the target quadrant as compared to the normal mice. The mice received DNPH of Isosteviol along in combination with D-gal spent significantly more time compared to D-gal treated mice in the target quadrant, but there spent time is less than the control mice (Fig. 6(B)).

To know the short memory recognition of the experimental mice Y-maze test was performed. In this test the percentage spontaneous alternation of the three mice groups was calculated through its respective formula. The results of Y-maze reveal that the percentage spontaneous alternation of control animals was very high while the D-gal mice showed a very low %age of spontaneous alternation. Interestingly, the third group of mice received DNPH of Isosteviol in combination with D-gal showed significantly higher percentage spontaneous alternation against only D-gal treated mice (Fig. 6(C)).



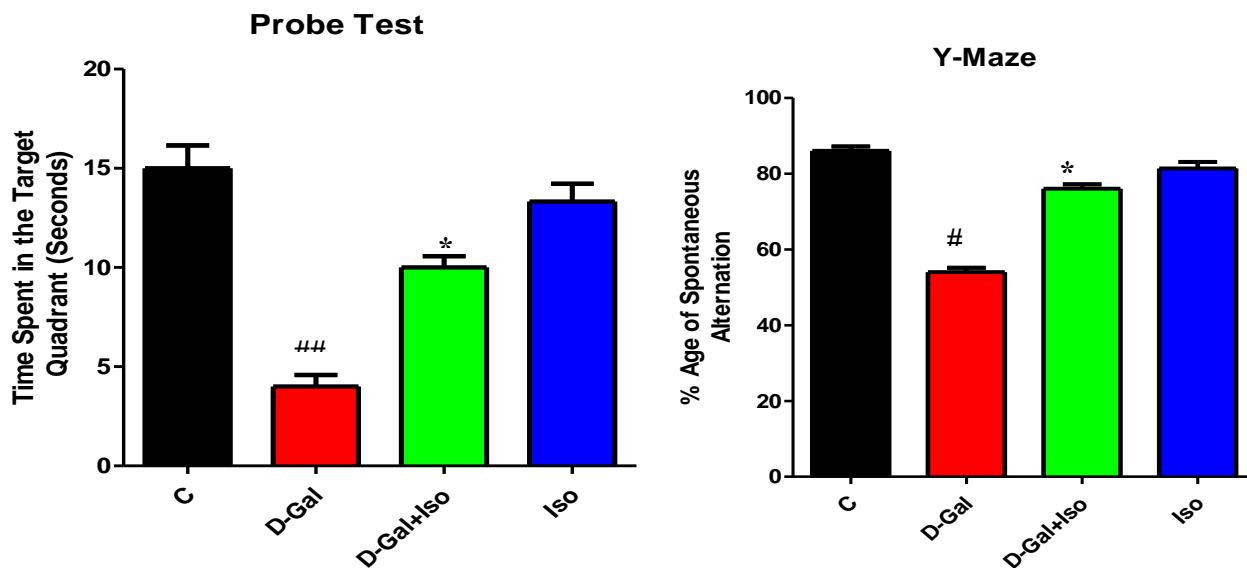


**Fig.6 DNPH of Isosteviol administration improved D-gal-induced memory dysfunction in adult mice.** All experimental groups underwent behavioral testing, notably the Morris water maze (MWM) and Y-maze. The histogram illustrates the average duration of escape delays (measured in seconds) during the MWM testing phase of the training process. The test results are exhibited continuously for a period of five days, specifically spanning from day 1 to day 5. The user's text is "(B)". The histogram shown illustrates the outcomes of the probe test carried out on the fifth day of the Morris Water Maze (MWM) experiment. This test specifically measures the duration of time spent in the target quadrant. The test was conducted with the submerged platform concealed. The histogram depicts the ratio of spontaneous behavior seen during the Y-maze test. The given data is displayed as the mean  $\pm$  standard error of the mean (S.E.M.). The data labeled with # indicates a statistically significant difference compared to the mice treated with normal saline, whereas the data labeled with \* indicates a statistically significant difference compared to the mice treated with D-gal. The data marked with ### indicates a significance level of  $P < 0.01$ .

## DISCUSSION

This study reports for the first time that DNPH of Isosteviol minimized the D-gal induced oxidative stress mediated neuroinflammation, synaptic dysfunction and memory impairment in animal model of aging. Most importantly, DNPH of Isosteviol directly activated SIRT1 which in turn stimulated NRF-2 and HO-1 proteins to limit the oxidative stress burden. Additionally, DNPH of Isosteviol inhibited TNF- $\alpha$  to reduce D-gal induced neuroinflammation and amyloidogenic pathway of A $\beta$  production in adult albino mice. Elegant studies have already documented that antioxidant agents either natural or synthetic are good drug candidates against D-gal-induced oxidative stress in the animal model of aging (Rusu *et al.*, 2019). While carrying out this study here, oxidative stress, neuroinflammation, synaptic dysfunction, and memory impairment—the four fundamental characteristics of D-galactose-induced aging—were our focus.

Oxidative stress occurs when there is an imbalance in the ratio between pro-oxidants and antioxidants, resulting in the generation of toxic reactive oxygen species (ROS) (Niedzielska *et al.*, 2016). The heightened oxidative stress induces neuroinflammation and neurodegeneration at the same time in age-related diseases like AD (Ikram *et al.*, 2019a) as well as Parkinson's disease and other animal models of neurodegeneration based on toxins (Khan *et al.*, 2019a; Badshah *et al.*, 2019). Several studies have revealed that D-galactose accelerates the aging process in animal models by inducing oxidative stress and neuroinflammation (Chang *et al.*, 2014). Multiple processes can lead to oxidative stress, including the suppression of endogenous ROS regulators and the activation of lipid peroxidation. During aging, there is a significant decline in the expression of SIRT1, which is critical for different neuronal survival by decreasing oxidative stress (Salminen *et*

*et al.*, 2013). Also, cells have an antioxidant defense system that is controlled by Nrf2. This system helps make proteins that are involved in oxidative stress and damage. When Nrf-2 is turned on, it targets many genes, including HO-1, that protect against oxidative stress, neuroinflammation, and cell death. This gives the brain a strong defense against neurodegeneration caused by oxidative stress (Johnson *et al.*, 2008).

This study found that DNPH and isosteviol therapy reduced the activity of  $\beta$ -Secretase (BACE1) and APP protein expression, hence inhibiting amyloidogenic A $\beta$  formation pathways. DNPH from isosteviol dramatically reduced A $\beta$  burden in adult albino mice's hippocampus. Evidence suggests that A $\beta$  synthesis and deposition lead to neuroinflammation, neurodegeneration, and memory impairment (Kumar *et al.*, 2015; Zhang *et al.*, 2015). NF-kB, a heterodimer molecule composed of p50 and p65 proteins, is an essential transcription factor (Berkowitz *et al.*, 2002). In this study, we demonstrated that DNPH of isosteviol suppressed NF-kB-mediated neuroinflammation. Isosteviol inhibits NF-kB DNPH, which in turn decreases downstream signalling molecules like TNF- $\alpha$  and IL-1 $\beta$ .

Here in the current study we evaluated the antioxidant capability of DNPH of Isosteviol, and our results reveal that DNPH of Isosteviol is one of the potent antioxidant agent. Here one thing should be noted that our western blot results shows that DNPH of Isosteviol is involved in the activation of SIRT1. It is that important endogenous target molecule which after activation, further stimulated the NRF-2/HO-1/TNF- $\alpha$  signaling pathway that minimized ROS production and its toxic effects and burden of the neuroinflammation against D-gal. DNPH of Isosteviol stimulated NRF2/HO-1 signaling pathway not only reduced the oxidative damage but also inhibited its downstream signaling to minimize the extent of neuroinflammation.

The predominant characteristics of the aging brain are synaptic dysfunction, diminished neural communication, and decreased release of neurotransmitters, resulting in reduced synaptic plasticity (Jellinger *et al.*, 2013). In age-related disorders like AD, there has been a lot of discussion regarding synaptic disruption (Ali *et al.*, 2018). But how exactly D-gal triggers synapse malfunction and neurological diseases is still a mystery. Elevated oxidative stress or the activation of inflammatory mediators can directly promote synaptic dysfunction, much as neuroinflammation can impair and synaptic functioning. In this study, our western blot analysis revealed that the administration of DNPH of Isosteviol increased the expression of both pre- and post-synaptic proteins in the brains of mice treated with D-gal. The findings of our work align with a prior investigation conducted by Latimer *et al.* (2014), which shown that DNPH of Isosteviol therapy increased the expression of many genes associated with both pre- and post-synaptic activity. Here in this study our western blot results shows that DNPH of Isosteviol administration enhanced expression of both pre-and post-synapse related proteins in D-gal treated mice brains. This is accompanied by DNPH of Isosteviol beneficial effect on the memory and behavior of aging animals. In the behavior test, DNPH of Isosteviol treated animals showed good performance both in the Morris water maze and Y-maze tests. The gradual decrease on each new day in mean escape latencies and spending more time (when submerged platform was hidden) in the target quadrant of DNPH of Isosteviol treated animals suggests that it plays a very vital role in improving impaired memory and cognition. Similarly, DNPH of Isosteviol treated mice also showed higher percentage spontaneous alternation in Y-maze test, reveals good effect of DNPH of Isosteviol on memory in mice.

Inflammation has a significant role in the course of dementia (Ikram *et al.*, 2020). Research indicates that D-gal promotes oxidative stress. Stress triggers both inflammatory and apoptotic cell death pathways (Rehman *et al.*, 2019). Furthermore, inflammatory responses are closely linked to oxidative stress. Oxidative stress can trigger the expression of inflammatory cytokines including IL-6 and IL-1 $\beta$ , leading to an inflammatory response. HO-1 is the enzyme that limits the rate of heme breakdown in the body to biliveric acid, Fe<sup>2+</sup>, and CO. Currently, cumulative research suggest that the Nrf2/HO-1 pathway is responsible for the regulation of inflammatory responses by reducing the amounts of inflammatory cytokines in organs such as the brain, liver, kidneys, etc.

To demonstrate the effects of DNPH of Isosteviol on high oxidative stress, we examined the expression of SIRT1, Nrf2, and HO-1 in the experimental groups, indicating that DNPH of Isosteviol effectively regulated elevated oxidative stress in D-galactose-injected mouse brains. As previously reported, SIRT1, Nrf-2, and HO-1 are downregulated in the brains of D-gal-treated mice (Chen *et al.*, 2019). The findings show that D-galactose-induced oxidative stress may be caused in part by the regulation of natural antioxidant systems, as previously suggested (Ahmad *et al.*, 2019). Interestingly, DNPH from isosteviol reduced oxidative stress, as evidenced by the ROS and LPO assays.

Sirtuins (SIRT1) are a class of histone deacetylases that rely on nicotinamide adenine dinucleotide (NAD<sup>+</sup>) and play a critical role in organ damage (Sosnowska *et al.*, 2017). It has been shown that SIRT1 can deacetylate p53 to reduce oxidative stress, apoptosis, and damage (Tian *et al.*, 2019). Furthermore, SIRT can increase Nrf2 expression while decreasing Bax expression (Wang *et al.*, 2021). Numerous investigations have shown that oxidative stress-induced apoptosis plays an important role in brain, liver, and renal injury, as well as a variety of senescence-related disorders (Kim *et al.*, 2014; Ullah *et al.*, 2018). Research indicates that apoptosis plays a significant role in the damage induced by D-gal (Zhang *et al.*, 2019). Furthermore, our docking results observed that the docking of DNPH in the allosteric binding site of SIRT1 obtained highest docking score of -3.2 kcal/mol, glide emodel score (-23.7kcal/mol) and glide energy (-18.3 kcal/mol). Such high docking energetics suggested that DNPH could feasibly interact and lodge in the allosteric binding site of SIRT1 and the resultant complex is highly stable. Conclusively, our docking results suggested that the most possible activation mechanism of DNPH is allosterically programmed which is also mechanistically confirmed by other studies (Dai *et al.*, 2015, Cao *et al.*, 2015).

Nrf2 is an important nuclear transcription factor that regulates the balance of oxidation and reduction in the body (Zhang *et al.*, 2024). Following the stimulation of ROS or oxidative stress production, Nrf2 is released from the Nrf2-Keap1-Cul3 complex and transferred into the nucleus to bind with the antioxidant response element (ARE), eventually promoting the transcription of various antioxidant enzymes (GSH-Px, CAT, SOD, and HO-1), GSH synthesis, and metabolism (Li *et al.*, 2023). These antioxidant enzymes serve critical roles in scavenging excess ROS. SOD catalyzes the conversion of O<sub>2</sub><sup>-</sup> into H<sub>2</sub>O<sub>2</sub>, which is then converted to H<sub>2</sub>O and oxygen via CAT catalysis (Gill *et al.*, 2013). Furthermore, GSH is the body's most abundant antioxidant, capable of directly scavenging free radicals, including lipid and metal radicals, via its unique redox processes catalyzed by GSH-Px and glutathione reductase (GR) (Yuan *et al.*, 2022). Thus, activating the Nrf2-regulated antioxidant pathway is critical for evaluating exogenous substances that stimulate the endogenous antioxidant potential. More specifically, our results from molecular docking confirmed that these chemicals could bind to the Nrf2 protein. In addition, our findings showed that DNPH of Isosteviol might activate the SIRT1/Nrf2/HO-1 pathway, improve antioxidant enzyme and TOC activity, promote GSH synthesis, and minimize ROS buildup.

As a result, the SIRT1/Nrf2/HO-1 pathway plays an important regulatory role in reducing D-gal-induced oxidative stress, inflammation, and apoptosis. Our findings revealed that Dinitrophenyl hydrazine (DNPH) of Isosteviol prevented apoptosis in D-gal-induced aging animals. Finally, the Western blot analysis results in this study showed that DNPH of Isosteviol might affect the protein expressions of SIRT1 and HO-1. These findings revealed that DNPH of Isosteviol therapeutic effect on age-related brain, liver, and kidney dysfunction was directly linked to the activation of the SIRT1 signal pathway.

Collectively our results suggested that DNPH of Isosteviol may attenuate oxidative stress, neuroinflammation, neurodegeneration, and memory impairment in D-gal treated mice via regulation of SIRT1, Nrf2/HO-1-mediated neuroinflammation. Our study is strongly supporting the previously conducted studies on the role of Isosteviol, Rosing *et al.*, 2020 finding point that Isosteviol Sodium (STVNA) has also *in vitro* neuroprotective effects at the Blood brain barrier (BBB).

Collectively, our findings demonstrate that the use of DNPH of Isosteviol effectively prevented the harmful effects associated with oxidative stress-induced neuroinflammation and Alzheimer's disease-like symptoms in an aging animal model. The recent findings precisely understand the signaling route of the neuroprotection provided by DNPH of Isosteviol in mice with D-gal-induced oxidative stress associated memory impairment.

## References

1. Fjell, A. M., Walhovd, K. B., Fennema-Notestine, C., McEvoy, L. K., Hagler Jr, D. J., Holland, D., Brewer, J. B., & Dale, A. M. (2014). Brain atrophy in healthy aging is related to CSF levels of A $\beta$ 1–42. *Cerebral Cortex*, *24*(5), 1215–1223.
2. Shwe, T., Pratchayasakul, W., Chattipakorn, N., & Chattipakorn, S. C. (2018). Role of D-galactose-induced brain aging and its potential used for therapeutic interventions. *Exp Gerontol*, *101*, 13-36.
3. Winklhofer, K. F., & Haass, C. (2010). Mitochondrial dysfunction in Parkinson's disease. *Biochimica et Biophysica Acta (BBA)-Molecular Basis of Disease*, *1802*(1), 29-44.
4. Arthur, C. R., Morton, S. L., Dunham, L. D., Keeney, P. M., & Bennett, J. P. (2009). Parkinson's disease brain mitochondria have impaired respirasome assembly, age-related increases in distribution of oxidative damage to mtDNA and no differences in heteroplasmic mtDNA mutation abundance. *Molecular neurodegeneration*, *4*(1), 1-13.
5. Carvalho, C., Correia, S. C., Santos, R. X., Cardoso, S., Moreira, P. I., Clark, T. A., ... & Perry, G. (2009). Role of mitochondrial-mediated signaling pathways in Alzheimer disease and hypoxia. *Journal of bioenergetics and biomembranes*, *41*, 433-440.
6. DeKosky, S. T., & Scheff, S. W. (1990). Synapse loss in frontal cortex biopsies in Alzheimer's disease: Correlation with cognitive severity. *Annals of Neurology*, *27*(5), 457-464.
7. Harada, C. N., Natelson Love, M. C., & Triebel, K. L. (2013). Normal cognitive aging. *Clinics in Geriatric Medicine*, *29*(4), 737-752
8. Zhao FF, Zhou YZ, Gao L, Qin XM, Du GH. (2017). [Advances in the study of the rat model of aging induced by D-galactose]. *Yao Xue Xue Bao*, *52*(3), 347-54. Chinese. PMID: 29979551.
9. Chen, L., Deng, H., Cui, H., Fang, J., Zuo, Z., Deng, J., ... & Yang, M. (2020). Inflammatory responses and inflammation-associated diseases in organs. *Oncotarget*, *9*(6), 7204.
10. Ren, Z., He, H., Zuo, Z., et al. (2019). The role of different SIRT1-mediated signaling pathways in toxic injury. *Cell Mol Biol Lett*, *24*, 36. <https://doi.org/10.1186/s11658-019-0158-9>
11. Zhang, X., Zhang, Q. X., Wang, X. M., Liu, L., & Dong, C. H. (2019). Effects of Iso Steviol on the oxidative stress and inflammation response in acute kidney injury induced by sepsis in rats. *Chinese Journal of Cellular and Molecular Immunology*, *35*(6), 585-590.
12. Hwang, J. W., Kim, S. J., Kim, Y. H., Seo, J. A., Kim, S. G., Kim, N. H., ... & Baik, S. H. (2021). Interaction of NRF2 and neuro-inflammatory factors predicts cognitive decline in elderly patients with type 2 diabetes. *Psychoneuroendocrinology*, *122*, 104927.
13. Chen C, Zhou M, Ge Y, Wang X. (2020). SIRT1 and aging related signaling pathways. *Mech Ageing Dev*, *187*, 111215. <https://doi.org/10.1016/j.mad.2020.111215>
14. Park, S. A., Kim, M. MY., & Kim, Y. S. (2021). The neuroprotective effects of Iso Steviol in primary cultures of rat cortical cells via the ROS-activated Erk1/2 and PI3K/Akt signaling pathways. *Food and Chemical Toxicology*, *146*, 111867.
15. Ullah, A., Munir, S., Mabkhot, Y., & Badshah, S. L. (2019). Bioactivity profile of the diterpene isosteviol and its derivatives. *Molecules*, *24*(4), 678.
16. Vorhees, C., Williams, M. Morris water maze: procedures for assessing spatial and related forms of learning and memory. *Nat Protoc* **1**, 848–858 (2006). <https://doi.org/10.1038/nprot.2006.116>



17. Kraeuter AK, Guest PC, Sarnyai Z. The Y-Maze for Assessment of Spatial Working and Reference Memory in Mice. *Methods Mol Biol.* 2019;1916:105-111. doi: 10.1007/978-1-4939-8994-2\_10. PMID: 30535688.
18. Zhang J, Chen R, Yu Z, Xue L. Superoxide Dismutase (SOD) and Catalase (CAT) Activity Assay Protocols for *Caenorhabditis elegans*. *Bio Protoc.* 2017 Aug 20;7(16):e2505. doi: 10.21769/BioProtoc.2505. PMID: 34541169; PMCID: PMC8413628.
19. Owen JB, Butterfield DA. Measurement of oxidized/reduced glutathione ratio. *Methods Mol Biol.* 2010;648:269-77. doi: 10.1007/978-1-60761-756-3\_18. PMID: 20700719.
20. Aguilar Diaz De Leon J, Borges CR. Evaluation of Oxidative Stress in Biological Samples Using the Thiobarbituric Acid Reactive Substances Assay. *J Vis Exp.* 2020 May 12;(159):10.3791/61122. doi: 10.3791/61122. PMID: 32478759; PMCID: PMC9617585.
21. de Oliveira FK, Santos LO, Buffon JG. Mechanism of action, sources, and application of peroxidases. *Food Res Int.* 2021 May;143:110266. doi: 10.1016/j.foodres.2021.110266. Epub 2021 Mar 5. PMID: 33992367.
22. McCord, J. M., & Fridovich, I. (1969). Superoxide dismutase: an enzymic function for erythrocyte hemoglobin. *Journal of Biological Chemistry*, 244(22), 6049-6055. McCord, J. M., & Fridovich, I. (1969). Superoxide dismutase: an enzymic function for erythrocyte hemoglobin. *Journal of Biological Chemistry*, 244(22), 6049-6055.
23. Fido, R.J., Tatham, A.S., Shewry, P.R. (1995). Western Blotting Analysis. In: Jones, H. (eds) *Plant Gene Transfer and Expression Protocols. Methods in Molecular Biology™*, vol 49. Springer, Totowa, NJ. <https://doi.org/10.1385/0-89603-321-X:423>
24. Rana RM, Rampogu S, Abid NB, Zeb A, *et al.*, (2020) In silico study identified methotrexate analog as potential inhibitor of drug resistant human dihydrofolate reductase for cancer therapeutics. *Molecules* 25 (15), 3510
25. Irfanullah, Amir Zeb, *et al.*, (2018) Molecular and in silico analyses validates pathogenicity of homozygous mutations in the NPR2 gene underlying variable phenotypes of Acromesomelic dysplasia, type Maroteaux. *The International Journal of Biochemistry & Cell Biology* 102, 76-86
26. Kumar, A., & Singh, A. (2015). A review on Alzheimer's disease pathophysiology and its management: an update. *Pharmacological reports*, 67(2), 195-203.
27. Parameshwaran K, Irwin MH, Steliou K, Pinkert CA. D-galactose effectiveness in modeling aging and therapeutic antioxidant treatment in mice. *Rejuvenation Res.* 2010 Dec;13(6):729-35. doi: 10.1089/rej.2010.1020. Epub 2011 Jan 4. PMID: 21204654; PMCID: PMC3034100.
28. Hammad, M., Raftari, M., Cesário, R., Salma, R., Godoy, P., Emami, S. N., & Haghdoost, S. (2023). Roles of oxidative stress and Nrf2 signaling in pathogenic and non-pathogenic cells: A possible general mechanism of resistance to therapy. *Antioxidants*, 12(7), 1371.
29. Shwe, T., Pratchayasakul, W., Chattipakorn, N., & Chattipakorn, S. C. (2018). Role of D-galactose-induced brain aging and its potential used for therapeutic interventions. *Experimental gerontology*, 101, 13-36.
30. Ahmad, S., Khan, A., Ali, W., Jo, M. H., Park, J., Ikram, M., & Kim, M. O. (2021). Fisetin rescues the mice brains against D-galactose-induced oxidative stress, neuroinflammation and memory impairment. *Frontiers in pharmacology*, 12, 612078.
31. Dai H, Case AW, Riera TV *et al.* Crystallographic structure of a small molecule SIRT1 activator-enzyme complex. *Nat. Comm.* 6 (2015), 7645
32. Cao D, Wang M, Qiu X *et al.* Structural basis for allosteric, substrate-dependent stimulation of SIRT1 activity by resveratrol. *Gene & Development.* 29 (2015), 1316-1325
33. Azminah A, Erlina L, Radji M *et al.* In silico and in vitro identification of candidate SIRT1 activators from Indonesian medicinal plants compounds database. 83 (2019), 107096.
34. Samad, N., Hafeez, F., & Imran, I. (2022). D-galactose induced dysfunction in mice hippocampus and the possible antioxidant and neuromodulatory effects of selenium. *Environmental Science and Pollution Research*, 29(4), 5718-5735.

35. Rusu, M. E., Mocan, A., Ferreira, I. C., & Popa, D. S. (2019). Health benefits of nut consumption in middle-aged and elderly population. *Antioxidants*, 8(8), 302.
36. Latimer, C. S., Brewer, L. D., Searcy, J. L., Chen, K. C., Popović, J., Kraner, S. D., ... & Porter, N. M. (2014). Vitamin D prevents cognitive decline and enhances hippocampal synaptic function in aging rats. *Proceedings of the National Academy of Sciences*, 111(41), E4359-E4366.
37. Niedzielska, E., Smaga, I., Gawlik, M. *et al.* Oxidative Stress in Neurodegenerative Diseases. *Mol Neurobiol* **53**, 4094–4125 (2016). <https://doi.org/10.1007/s12035-015-9337-5>
38. Ikram, M., Muhammad, T., Rehman, S. U., Khan, A., Jo, M. G., Ali, T., *et al.* (2019a). Hesperetin confers neuroprotection by regulating nrf2/TLR4/NFkappaB signaling in an abeta mouse model. *Mol. Neurobiol.* 56(9), 6293–6309. doi:10.1007/s12035-019-1512-7
39. Khan, A., Ikram, M., Muhammad, T., Park, J., and Kim, M. O. (2019a). Caffeine modulates cadmium-induced oxidative stress, neuroinflammation, and cognitive impairments by regulating nrf-2/HO-1 in vivo and in vitro. *J. Clin. Med.* 8(5), 680. doi:10.3390/jcm8050680
40. Badshah, H., Ikram, M., Ali, W., Ahmad, S., Hahm, J. R., and Kim, M. O. (2019). Caffeine may abrogate LPS-induced oxidative stress and neuroinflammation by regulating nrf2/TLR4 in adult mouse brains. *Biomolecules* 9(11), 719. doi:10.3390/biom9110719
41. Chang, L., Liu, X., Liu, J., Li, H., Yang, Y., Liu, J., *et al.* (2014). D-galactose induces a mitochondrial complex I deficiency in mouse skeletal muscle: potential benefits of nutrient combination in ameliorating muscle impairment. *J. Med. Food* 17, 357–364. doi:10.1089/jmf.2013.2830
42. Salminen, A., Kaarniranta, K., and Kauppinen, A. (2013). Crosstalk between oxidative stress and SIRT1: impact on the aging process. *Int. J. Mol. Sci.* 14, 3834–3859. doi:10.3390/ijms14023834
43. Johnson, J. A., Johnson, D. A., Kraft, A. D., Calkins, M. J., Jakel, R. J., Vargas, M. R., *et al.* (2008). The Nrf2-ARE pathway: an indicator and modulator of oxidative stress in neurodegeneration. *Ann. N. Y. Acad. Sci.* 1147, 61–69. doi:10.1196/annals.1427.036
44. Ahmad, A., Ali, T., Rehman, S. U., and Kim, M. O. (2019). Phytomedicine-based potent antioxidant, fisetin protects CNS-insult LPS-induced oxidative stress-mediated neurodegeneration and memory impairment. *J. Clin. Med.* 8(6), 850. doi:10.3390/jcm8060850
45. Chen, P., Chen, F., and Zhou, B. H. (2019). Leonurine ameliorates D-galactose-induced aging in mice through activation of the Nrf2 signalling pathway. *Aging* 11, 7339–7356. doi:10.18632/aging.101733
46. Ikram, M., Ullah, R., Khan, A., and Kim, M. O. J. C. (2020). Ongoing research on the role of gintonin in the management of neurodegenerative disorders. *Cells*, 9, 1464. doi:10.3390/cells9061464
47. Rehman, S. U., Ikram, M., Ullah, N., Alam, S. I., Park, H. Y., Badshah, H., *et al.* (2019). Neurological enhancement effects of melatonin against brain injury-induced oxidative stress, neuroinflammation, and neurodegeneration via AMPK/CREB signaling. *Cells* 8(7), 760. doi:10.3390/cells8070760
48. Tian, Y., Wen, Z., Lei, L., Li, F., Zhao, J., Zhi, Q., ... & Ming, J. (2019). Coreopsis tinctoria flowers extract ameliorates D-galactose induced aging in mice via regulation of Sirt1-Nrf2 signaling pathway. *Journal of functional foods*, 60, 103464.
49. Sosnowska, B., Mazidi, M., Penson, P., Gluba-Brzózka, A., Rysz, J., & Banach, M. (2017). The sirtuin family members SIRT1, SIRT3 and SIRT6: Their role in vascular biology and atherogenesis. *Atherosclerosis*, 265, 275-282.
50. Wang, W., Liu, F., Xu, C., Liu, Z., Ma, J., Gu, L., ... & Hou, J. (2021). Lactobacillus plantarum 69-2 combined with galacto-oligosaccharides alleviates d-galactose-induced aging by regulating the AMPK/SIRT1 signaling pathway and gut microbiota in mice. *Journal of Agricultural and Food Chemistry*, 69(9), 2745-2757.

51. Kim, M., Cho, K. H., Shin, M. S., Lee, J. M., Cho, H. S., Kim, C. J., ... & Yang, H. J. (2014). Berberine prevents nigrostriatal dopaminergic neuronal loss and suppresses hippocampal apoptosis in mice with Parkinson's disease. *International Journal of Molecular Medicine*, 33(4), 870-878.
52. Ullah, F., Ali, T., Ullah, N., & Kim, M. O. (2015). Caffeine prevents d-galactose-induced cognitive deficits, oxidative stress, neuroinflammation and neurodegeneration in the adult rat brain. *Neurochemistry international*, 90, 114-124.
53. Zhang, X., Wu, J. Z., Lin, Z. X., Yuan, Q. J., Li, Y. C., Liang, J. L., ... & Liu, Y. H. (2019). Ameliorative effect of supercritical fluid extract of *Chrysanthemum indicum* Linné against D-galactose induced brain and liver injury in senescent mice via suppression of oxidative stress, inflammation and apoptosis. *Journal of ethnopharmacology*, 234, 44-56.
54. Zhang, L., Xu, L. Y., Tang, F., Liu, D., Zhao, X. L., Zhang, J. N., ... & Ao, H. (2024). New perspectives on the therapeutic potential of quercetin in non-communicable diseases: Targeting Nrf2 to counteract oxidative stress and inflammation. *Journal of Pharmaceutical Analysis*.
55. Li, A., Chen, S., Yang, Z., Luan, C., Lu, W., Hao, F., ... & Wang, D. (2023). 4-Methylguaiacol alleviated alcoholic liver injury by increasing antioxidant capacity and enhancing autophagy through the Nrf2-Keap1 pathway. *Food Bioscience*, 51, 102160.
56. Gill, T., & Levine, A. D. (2013). Mitochondria-derived hydrogen peroxide selectively enhances T cell receptor-initiated signal transduction. *Journal of Biological Chemistry*, 288(36), 26246-26255.
57. Yuan, Y., Yucai, L., Lu, L., Hui, L., Yong, P., & Haiyang, Y. (2022). Acrylamide induces ferroptosis in HSC-T6 cells by causing antioxidant imbalance of the XCT-GSH-GPX4 signaling and mitochondrial dysfunction. *Toxicology Letters*, 368, 24-32.
58. Ali, T., Kim, T., Rehman, S. U., Khan, M. S., Amin, F. U., Khan, M., ... & Kim, M. O. (2018). Natural dietary supplementation of anthocyanins via PI3K/Akt/Nrf2/HO-1 pathways mitigate oxidative stress, neurodegeneration, and memory impairment in a mouse model of Alzheimer's disease. *Molecular neurobiology*, 55, 6076-6093.
59. Al-Rasheed NM Al-Rasheed NM Bassiouni YA Hasan IH Al-Amin MA Al-Ajmi HN et al. (2015) Vitamin D attenuates pro-inflammatory TNF- $\alpha$  cytokine expression by inhibiting NF- $\kappa$ B/p65 signaling in hypertrophied rat hearts. *J Physiol Biochem* 71(2): 289–299
60. Berkowitz, B., Huang, D. B., Chen-Park, F. E., Sigler, P. B., & Ghosh, G. (2002). The X-ray crystal structure of the NF- $\kappa$ B p50· p65 heterodimer bound to the interferon  $\beta$ - $\kappa$ B site. *Journal of Biological Chemistry*, 277(27), 24694-24700.